Penetration through Slots in Cylindrical Cavities Operating at Fundamental Cavity Modes in the Presence of Electromagnetic Absorbers

Salvatore Campione*, **Larry K. Warne, Isak C. Reines,**
Roy K. Gutierrez, and Jeffery T. Williams

Abstract—Placing microwave absorbing materials into a high-quality factor resonant cavity may in general reduce the large interior electromagnetic fields excited under external illumination. In this paper, we aim to combine two analytical models we previously developed: 1) an unmatched formulation for frequencies below the slot resonance to model shielding effectiveness versus frequency; and 2) a perturbation model approach to estimate the quality factor of cavities in the presence of absorbers. The resulting model realizes a toolkit with which design guidelines of the absorber's properties and location can be optimized over a frequency band. Analytic predictions of shielding effectiveness for three transverse magnetic modes for various locations of the absorber placed on the inside cavity wall show good agreement with both full-wave simulations and experiments, and validate the proposed model. This analysis opens new avenues for specialized ways to mitigate harmful fields within cavities.

1. INTRODUCTION

Electrical circuits and systems often require protection against unwanted interactions with harsh external electromagnetic (EM) environments. This protection is generally provided through electromagnetic shielding and may take the form of an enclosure, such as a metallic cavity, which may allow external EM fields to penetrate the interior of the cavity. This enclosure may support resonances with high-quality factor, which may lead to very large interior field levels [1–8]. These large fields could in turn be harmful to circuits and systems therein. Shielding effectiveness, defined as $\mathrm{SE}(\mathbf{r}) = |\mathbf{E}_{\mathrm{cavity}}(\mathbf{r})|/E_0$, with $\mathbf{E}_{\mathrm{cavity}}(\mathbf{r})$ the field inside the cavity at location $\mathbf{r}$ and E_0 the external incident electric field strength, is a quantity that measures the shielding performance of an enclosure. Placing microwave absorber materials within the enclosure may reduce such large fields and provide additional means for the protection of electrical systems [6, 7, 9, 10].

In this paper, we aim to model analytically EM absorbing material placement within a slotted cylindrical cavity to dampen the internal fields. In particular, we aim to combine two analytical models we previously developed to provide shielding effectiveness versus frequency at resonant modes in the presence of microwave absorber materials: 1) an unmatched formulation to model shielding effectiveness versus frequency [8]; and 2) a perturbation model approach to estimate the quality factor of cavities in the presence of absorbers [7]. It is important to point out that the first model provides shielding effectiveness spectra only for an empty cavity, while the second model only provides the quality factor change when an absorber is introduced within the cavity (and no shielding effectiveness spectra). Thus, the analysis here reported is necessary to validate and investigate the appropriateness of a model to analyze cavities loaded with absorber materials.

As mentioned in [10], there is a lack of analytic tools to determine the optimum absorber properties and placement; our resulting model represents a design toolkit that will be used in future work to optimize the absorber's properties and location over a frequency band, opening new avenues to maximize the interior cavity real-estate while simultaneously reducing large fields that may adversely affect the electronics' electrical performance and reliability.

2. SAMPLE ENCLOSURE: SLOTTED CYLINDRICAL CAVITY LOADED WITH AN ABSORBER MATERIAL

We consider here the enclosure in Fig. 1: a slotted, 0.25 inch thick cylindrical cavity made of aluminum-alloy with conductivity $\sigma = 2.6 \times 10^7$ S/m, interior height $h = 24$ inch $= 60.96$ cm, and interior radius $a = 4$ inch $= 10.16$ cm. The slot is azimuthally located on one side of the cylinder, midway along the cylinder height as shown in Fig. 1(a), with a width $w = 0.02$ inch $= 5.08 \times 10^{-4}$ m and a length $\ell = 2a \sin^{-1}[\ell_p/(2a)] \approx 2.02$ inch $= 5.13$ cm ($\ell_p = 2$ inch $= 5.08$ cm is the projected length). At the frequencies here analyzed below its resonance of 2.92 GHz, the slot acts as a magnetic current source drive for the interior cavity modes from the exterior fields. We consider the three absorber locations shown in Figs. 1(b)–(d), which are referred to as 'Case 1', 'Case 2', and 'Case 3', with the following center absorber locations: $z = 0$ (Case 1), $z = -h/6$ (Case 2), and $z = -h/4$ (Case 3).
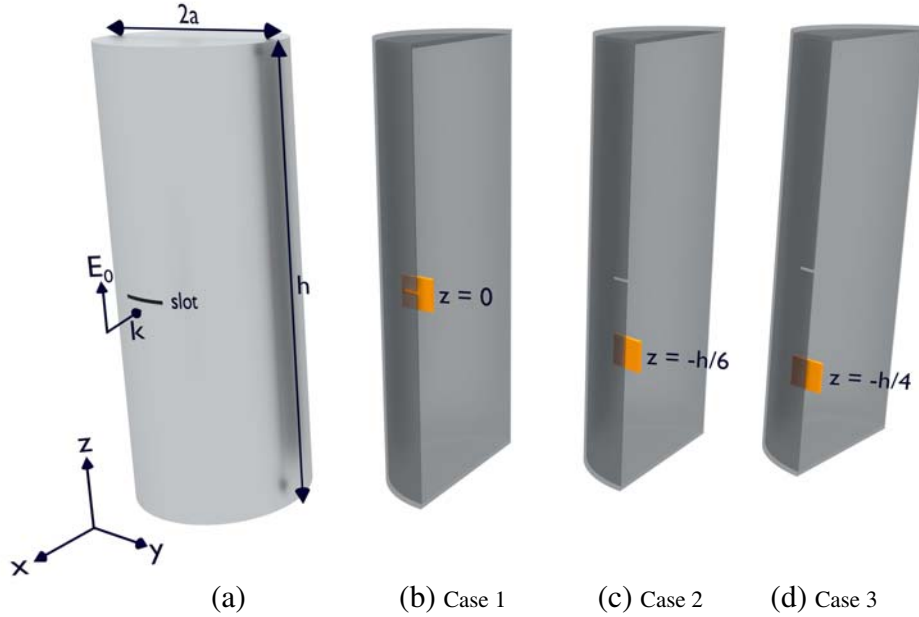

Figure 1. (a) Schematic of a slotted cylindrical enclosure excited by a plane-wave incident field as depicted to probe TM modes. The cavity is loaded with a microwave absorber material (orange box) at three different positions as outlined in panels (b)–(d) to dampen the EM fields. The origin of the reference system is at the center of the cylinder.

3. UNMATCHED FORMULATION FOR A LOADED CYLINDRICAL CAVITY

The cylindrical enclosure in Fig. 1 supports transverse magnetic (TM) and transverse electric (TE) modes [6, 8, 11, 12]. We focus on TM modes here, and briefly summarize the analytical, unmatched formulation to calculate the shielding effectiveness versus frequency around cavity modes reported in [8], and modify it to allow for the modeling of cavities loaded with absorber materials. We focus on slot

apertures operating below their resonant frequency; the case of slots operating at or above their resonant frequency will be considered in future work.

Under time dependence $\exp(-i\omega t)$, for empty, fully-enclosed cylindrical cavities with internal height h and internal radius a, following [6, 8, 11, 12], the interior magnetic resonant fields for fundamental TM modes even in z with indices (m, p, n) in space for $0 < \phi < 2\pi$, $0 < \rho < a$, $-h/2 < z < h/2$ are

$$H_\rho = \frac{i\omega\varepsilon_0}{\varsigma_{m,p,n}^2}\frac{m}{\rho}A_{m,p,n}J_m\left(\varsigma_{m,p}\rho\right)\sin\left(m\phi\right)\cos\left(\alpha_n z\right),$$

$$H_\varphi = \frac{i\omega\varepsilon_0}{\varsigma_{m,p,n}^2}\varsigma_{m,p}A_{m,p,n}J_m'\left(\varsigma_{m,p}\rho\right)\cos\left(m\phi\right)\cos\left(\alpha_n z\right),$$

(1)

with $k_{m,p,n} = \omega_{m,p,n}\sqrt{\mu_0\varepsilon_0} = \sqrt{\varsigma_{m,p}^2 + \alpha_n^2}$, $\alpha_n = n\pi/h$, $\varsigma_{m,p} = j_{m,p}/a$, $j_{m,p}$ the zeroes of the Bessel function of first kind $J_m(\rho)$ of order m, $\varsigma_{m,p,n} = \sqrt{k_{m,p,n}^2 - \alpha_n^2}$, μ_0 the permeability of free space, ε_0 the permittivity of free space, $p = 1, 2, ..., n = 0, 1, 2, ...$, and

$$A_{m,p,n} = -\frac{4\varepsilon_n\varepsilon_m}{3\pi h b}\frac{\ell}{2}\frac{V(0)\cos(m\phi_s)}{1-\frac{2}{5}(0.5k_{m,p,n}\ell)^2}\frac{1}{j_{m,p}J_{m-1}(j_{m,p})}\frac{k_{m,p,n}^2 - (n\pi/h)^2}{k^2 + kk_{m,p,n}(1+i)/Q_{m,p,n}^{\text{total}} - k_{m,p,n}^2}\cos(n\pi z_s/h)$$

(2)

are coefficients that account for the coupling through the voltage $V(0)$ connected to the exterior short circuit current density at the center of the slot, and ϕ_s and z_s depict the location of the slot. Furthermore, the term k depicts the free space wavenumber with which we are able to model frequency dispersion around cavity resonant modes. Note that because we consider a cavity loaded with an absorber material here, the term $Q_{m,p,n}^{\text{total}}$ appears in Eq. (2) rather than the quality factor of a mode supported by an empty cavity $Q_{m,p,n}^{\text{cavity}}$ as reported in [8]. This is not a trivial change that requires to be validated via experiments, as we do in this paper.

Assuming a dense and with limited volume microwave absorber material, with absolute permittivity ε_m and absolute permeability μ_m, the quality factor $Q_{m,p,n}^{\text{total}}$ can be estimated using perturbation theory [7, 12] via

$$Q_{m,p,n}^{\text{total}} = \left(\frac{1}{Q_{m,p,n}^{\text{cavity}}} + \frac{1}{Q_{m,p,n}^{\text{absorber}}}\right)^{-1}$$

(3)

where $Q_{m,p,n}^{\text{cavity}} = \eta\sqrt{j_{m,p}^2 + \alpha_n^2 a^2}/[2R_S(1 + \varepsilon_n a/h)]$, $\eta = \sqrt{\mu_0/\varepsilon_0}$, $\varepsilon_n = 1$ if $n = 0$, and $\varepsilon_n = 2$ if $n \neq 0$, and $R_S = \sqrt{\omega\mu_0/(2\sigma)}$ is the surface resistance, and

$$Q_{m,p,n}^{\text{absorber}} \approx \omega_{m,p,n}\frac{\iiint_V \mu_0|\mathbf{H}_0|^2\,dV}{\oiint_S R|\mathbf{H}_0|^2\,dS},$$

(4)

is the quality factor associated with losses of the absorber material, where the field $|\mathbf{H}_0| = |H_\rho\boldsymbol{\rho} + H_\varphi\boldsymbol{\varphi}|$ is assumed to be the one of the unperturbed cavity as in Eq. (1) (in other words, the fields of the loaded cavity are assumed to be only slightly different from the unperturbed, empty cavity model). Furthermore, $\omega_{m,p,n}$ is the modal resonance angular frequency; $R = \text{Re}[-iZ_m\tan(k_m d)]$ is the absorber surface resistance; $Z_m = \sqrt{\mu_m/\varepsilon_m}$ is the absorber impedance; $k_m = \omega\sqrt{\varepsilon_m\mu_m}$ is the wavenumber in the absorber material; and d is the absorber thickness.

The interior resonant z-component of the electric field for TM modes used to compute shielding effectiveness is given by

$$E_z = A_{m,p,n}J_m\left(\varsigma_{m,p}\rho\right)\cos\left(m\phi\right)\cos\left(\alpha_n z\right).$$

(5)

Maps of the magnitude of the normalized electric and magnetic fields in the x-z plane within an empty cavity at $y = 0$ for the TM_{012} mode resonating at about 1.232 GHz are reported in Fig. 2; one can note the presence of two maxima and two minima within the cavity along the z direction. Note
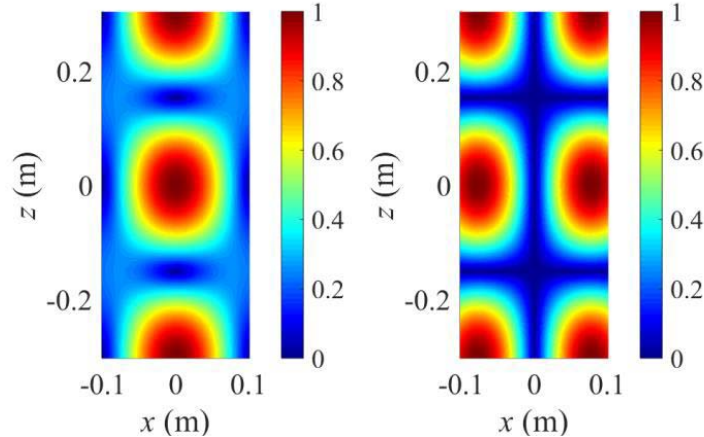
Figure 2. Normalized electric and magnetic field magnitude maps for the TM_{012} mode in an empty cavity in the x-z plane for $y = 0$ from Eqs. (1) and (5).

that the absorber will be placed at a vertical cavity wall, where in general the electric field exhibits low values. However, the magnetic field map is pivotal in determining the effect of the absorber depending on its location within the cavity as shown in the next section.

4. ANALYSIS OF SHIELDING EFFECTIVENESS IN CAVITIES LOADED WITH ABSORBER MATERIALS

The absorber we consider here is the commercial material ECCOSORB MCS absorber material [13], a thin, flexible, high-loss, magnetically loaded, electrically non-conductive broadband silicone absorber, with thickness $d = 1$ mm, radial extent of 3.181 inch (about 8.08 cm), and width along z of 1.201 inch (about 3.05 cm) (totaling 0.013% of the cavity volume), whose permittivity and permeability in the band 1–3 GHz can be approximated by $\varepsilon_m = \varepsilon_0(38 + i1)$ and $\mu_m = \mu_0(4.5 + i3)$, respectively. We consider the three absorber locations shown in Figs. 1(b)–(d): Case 1 aligns with the maximum magnetic field in Fig. 2; Case 2 falls midway between the maximum and minimum magnetic field; Case 3 aligns with the minimum magnetic field. We chose these three cases to validate the analytical model and to highlight how the position of the absorber greatly affects the interior field reduction, especially over a frequency band. Optimization of the absorber material properties and cavity placement will be investigated in future work leveraging the model discussed in this paper.

The quality factors for an empty cavity as well as the three loaded cavities in Figs. 1(b)–(d) for the TM_{012} mode are reported in Table 1: one can see that while Cases 1 and 2 have largely reduced quality factors with respect to the empty case, this is not observed for Case 3. Indeed, Case 3 exhibits the absorber near a minimum of the magnetic field (see Fig. 2), and thus does little to dampen the fields within the cavity.

Table 1. Quality factors for the empty and loaded cavities in Fig. 1 for the TM_{012} mode.

Case	$Q_{m,p,n}^{\text{total}}$	$Q_{m,p,n}^{\text{cavity}}/Q_{m,p,n}^{\text{total}}$
Empty	27095	1.00
1	1191.5	22.74
2	4124	6.57
3	22948	1.18

Using Eqs. (2) and (3) in the field Eq. (5), one can compute shielding effectiveness from the unmatched formulation in the presence of the absorber at $\mathbf{r} = (2.54\,\text{cm}, 180°, -h/2 + 0.43\,\text{cm})$, which is reported in Fig. 3 for the three absorber locations considered in Figs. 1(b)–(d) as well as for an empty
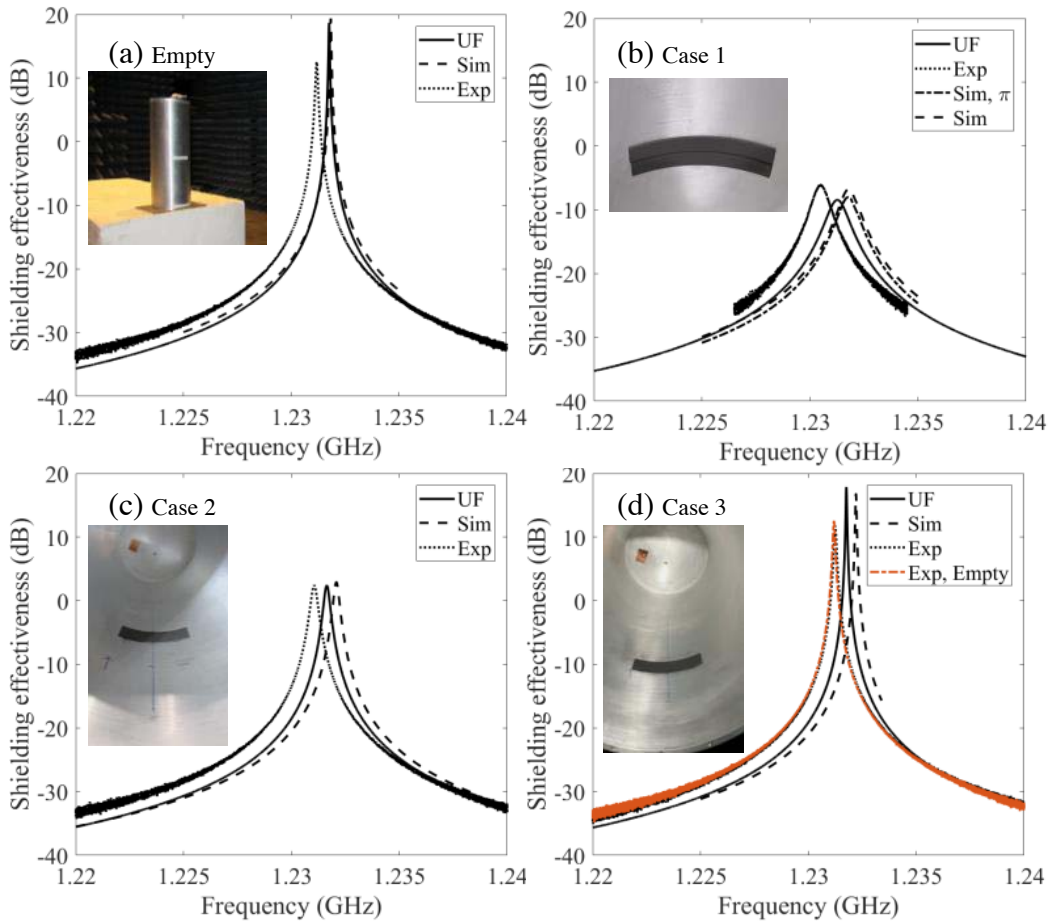
Figure 3. Shielding effectiveness versus frequency for the TM_{012} mode for (a) an empty cavity, and a loaded cavity as in (b) Case 1, (c) Case 2, and (d) Case 3. Photos of experiments are reported as insets. The unmatched formulation (UF) results using the short circuit current density for a finite cylinder are reported as solid curves. Full-wave simulation (Sim) and experimental (Exp) results are reported as dashed and dotted curves, respectively. The x-axis scale is narrow (1.22 to 1.24 GHz) around the TM_{012} mode to capture the exhibited large quality factors.

cavity (note shielding effectiveness is shown in dB units). These results are compared in Fig. 3 to full-wave simulations and experimental data. Our measurements were performed in an anechoic chamber on the test cylinder reported in the insets of Fig. 3 placed 3 m from the antenna and aligned to have the aperture slot at the same height as the transmitting antenna; we used a 4.3 mm monopole (designed to have negligible effect on the cavity performance) located on one plate of the cylinder and placed 1" off center. We used a 4-port network analyzer located outside the anechoic chamber to both supply and monitor the RF signal while also measuring the monopole field level. A wide band 10–4200 MHz mini-circuits power amplifier is used to boost the RF signal from the network analyzer before the signal is transmitted using a 30 MHz to 6 GHz Biconilog antenna with the electric field oriented along the axis of the cylinder. In a separate measurement, an AD80D field sensor is placed in the same location as the test cylinder aperture slot to measure the incident field level which is required for the shielding effectiveness normalization.

One can see that analytics, simulations, and experiments are in good agreement in terms of spectral position, quality factor, and shielding effectiveness peak value, validating the proposed model. For Case 3 and the empty cavity, the small discrepancies between experiments and full-wave simulations are due to additional joint losses as discussed in [6]; these additional losses are negligible in the presence of an absorber that dampens the resonances as in Cases 1 and 2. In particular, the modeled peak shielding
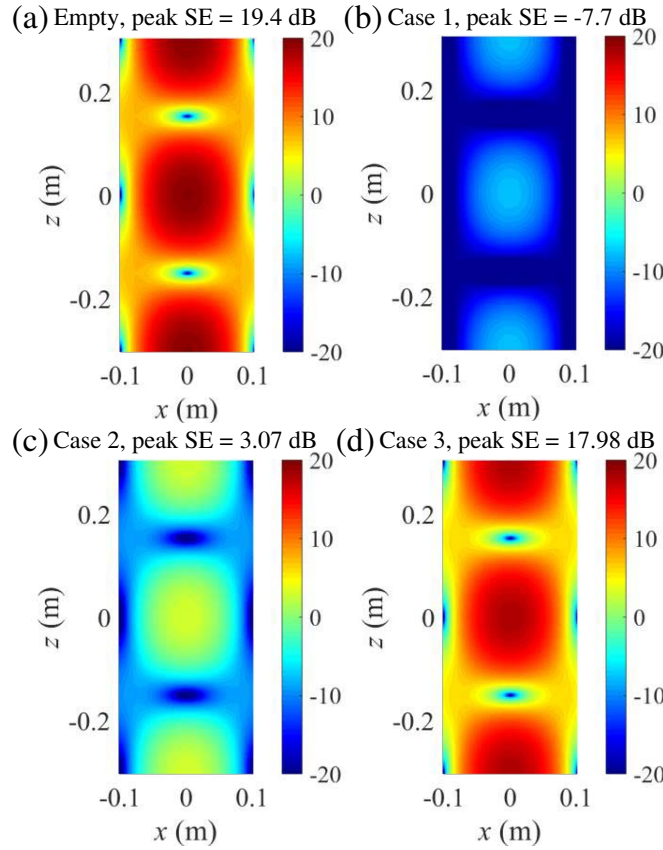
Figure 4. Electric field magnitude maps for the TM_{012} mode for (a) an empty cavity, and a loaded cavity as in (b) Case 1, (c) Case 2, and (d) Case 3. in the x-z plane for $y = 0$. SE is the abbreviation used for shielding effectiveness.

effectiveness is about: 18.7 dB for the empty cavity, 17.9 dB for Case 3, 2.4 dB for Case 2, and -8.5 dB for Case 1, showing a maximum improvement of shielding effectiveness of about 27 dB for this mode when the absorber is placed at a magnetic field maximum. Note similar results would be obtained if the absorber were azimuthally shifted by a π phase at each respective location (see the result for Case 1 in Fig. 3(b)). Although we are moving the absorber in azimuth, we are still maintaining the same modal symmetry by selecting a position of π with respect to the slot. Fig. 3 confirms that the unmatched formulation here presented works well also in the presence of absorbers within the cavity, even for the case when there is a twentyfold reduction in quality factor (Case 1). Furthermore, it also confirms that introducing an absorber within the cavity does not necessarily guarantee an improvement of shielding effectiveness, as attested by the result of Case 3 (note that the experimental result in Fig. 3(d) nearly overlaps with the empty cavity result). In other words, this stresses the fact that inserting localized absorbers within the cavity may not necessarily lead to reduced fields due to field nulls and mode degeneracies.

Though in the experiments we are limited to sample the field at one probe in space within the cavity, we can now use the validated model to investigate the spatial distribution of interior field levels within the cavity. Maps of the magnitude of the electric field in the x-z plane at $y = 0$ for the four cases in Fig. 3 are reported in Fig. 4. One can see that while the field distribution is very similar in all cases, the magnitude is largely dependent on the position of the absorber within the cavity; overall, one can see that the entire field distribution is affected by a single absorber at one location in space, with Case 1 showing the largest field reduction in the cavity.

We also investigate the effect of the absorber positions in Figs. 1(b)–(d) for two other modes supported by the cavity in Fig. 5: the TM_{010} and the TM_{114} (note that by approaching the slot
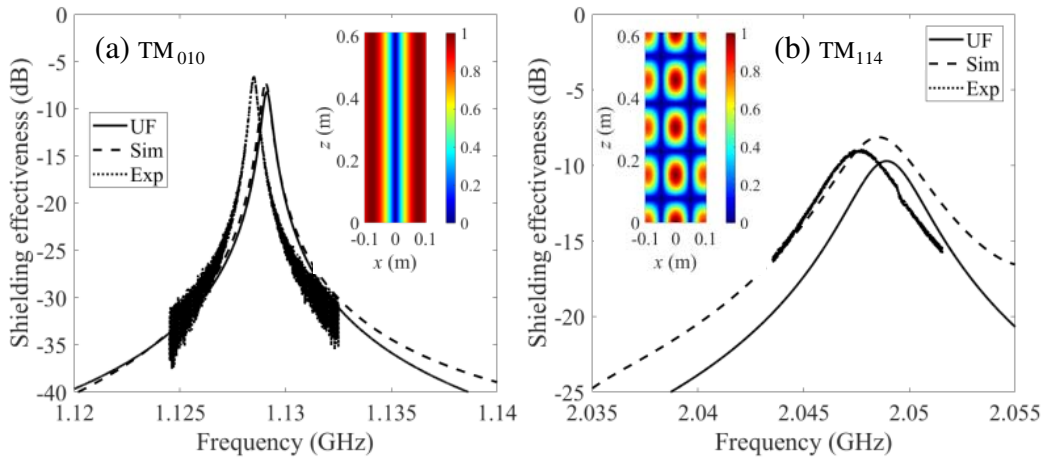
Figure 5. Shielding effectiveness versus frequency for the (a) TM_{010} and (b) TM_{114} modes for a loaded cavity with an absorber located at a magnetic field peak. Normalized magnetic field magnitude distribution within the cavity in the x-z plane for $y = 0$ from Eq. (1) for the two cases are reported as insets.
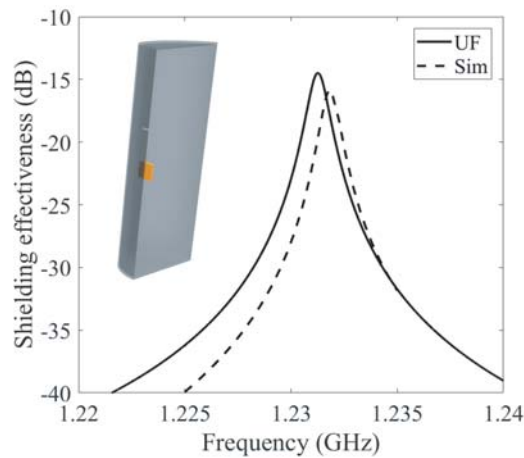

Figure 6. Shielding effectiveness versus frequency for the TM_{012} mode for a slotted cavity with a slot located at $z = h/6$ with an absorber at $z = 0$. The absorber location within the cavity is reported as inset.

resonance for increasing frequency, the unmatched formulation becomes less accurate). Regarding the TM_{010} mode, since the magnetic field is maximum along the entire wall surface (see inset of Fig. 5(a)), all the absorber locations considered in Fig. 1 lead to a quality factor of about 2309, resulting in a shielding effectiveness peak of about -8.2 dB. The situation is different for the TM_{114} mode: the absorber locations at $z = 0$ and $z = -h/4$ align with magnetic field peaks, leading to a quality factor of about 573 and peak shielding effectiveness of about -9.7 dB. The absorber location at $z = -h/6$ aligns with a medium level magnetic field (see inset of Fig. 5(b)), leading to a quality factor of about 1996 and peak shielding effectiveness of about 1.1 dB (not shown). The unmatched formulation results shown in Fig. 5 are in agreement with both full-wave simulation and experimental results. Importantly, for the three modes here considered, one can note that the absorber location and material properties in conjunction with the magnetic field profile in the cavity are pivotal in improving shielding effectiveness, and an optimization over a frequency band will be required for improved wideband performance.

We finally consider the case where the slot is located at $z = h/6$ in Fig. 6 and investigate the absorber location at $z = 0$ in correspondence of the magnetic field peak. Although modes that have odd parity for the H field can be generated, they are not degenerate in frequency. In addition to the

shielding effectiveness improvement due to the alignment of the absorber with the magnetic field peak, an additional improvement is provided by misaligning the slot from the field maximum, as observed by comparing Fig. 3(b) and Fig. 6. This confirms further that the absorber location for optimal dampening of fields within the cavity is of critical importance.

5. CONCLUSION

We discussed in this paper an analytical model that estimates the shielding effectiveness of cavities in the presence of absorbers. This model combines: 1) an unmatched formulation to model shielding effectiveness versus frequency; and 2) a perturbation model approach to evaluate the quality factor of cavities in the presence of absorbers. Comparisons of results for three transverse magnetic modes from this model to both full-wave simulations and experiments were performed for various locations of the absorber within the cavity. Importantly, the absorber location relative to the magnetic field magnitude distribution within the cavity is pivotal to maximizing shielding effectiveness improvements. These results showed good agreement and validated the proposed model, which can then be used as a toolkit to optimize the absorber's properties and location over a frequency band for shielding effectiveness improvement. Reducing interior field levels using absorbers allows for a more seamless protection of electrical circuits and systems contained within the cavity.

ACKNOWLEDGMENT

REFERENCES

1. Robinson, M. P., et al., "Analytical formulation for the shielding effectiveness of enclosures with apertures," *IEEE Transactions on Electromagnetic Compatibility*, Vol. 40, No. 3, 240–248, 1998.
2. Nie, X.-C. and N. Yuan, "Accurate modeling of monopole antennas in shielded enclosures with apertures," *Progress In Electromagnetics Research*, Vol. 79, 251–262, 2008.
3. Eng Swee, S., et al., "Coupling studies and shielding techniques for electromagnetic penetration through apertures on complex cavities and vehicular platforms," *IEEE Transactions on Electromagnetic Compatibility*, Vol. 45, No. 2, 245–257, 2003.
4. Tait, G. B., et al., "On measuring shielding effectiveness of sparsely moded enclosures in a reverberation chamber," *IEEE Transactions on Electromagnetic Compatibility*, Vol. 55, No. 2, 231–240, 2013.
5. Warne, L. K., et al., "A bound on electromagnetic penetration through a slot aperture with backing cavity," *Sandia National Laboratories Report, 2016*, SAND2016-9029, Albuquerque, NM, USA, 2016.
6. Campione, S., et al., "Preliminary survey on the effectiveness of an electromagnetic dampener to improve system shielding effectiveness," *Sandia National Laboratories Report, 2018*, SAND2018-10548, Albuquerque, NM, 2018.
7. Campione, S., et al., "Perturbation theory to model shielding effectiveness of cavities loaded with electromagnetic dampeners," *Electronics Letters*, Vol. 55, No. 11, 644–646, 2019.

8. Campione, S., et al., "Penetration through slots in cylindrical cavities operating at fundamental cavity modes," *IEEE Transactions on Electromagnetic Compatibility*, doi: 10.1109/TEMC.2020.2977600, 2020.

9. Williams, D. F., "Damping of the resonant modes of a rectangular metal package [MMICs]," *IEEE Transactions on Microwave Theory and Techniques*, Vol. 37, No. 1, 253–256, 1989.

10. Dixon, P., "Cavity-resonance dampening," *IEEE Microwave Magazine*, Vol. 6, No. 2, 74–84, 2005.

11. Campione, S., et al., "Antenna loading impact on the coupling response of a slotted cylindrical cavity," *Sandia National Laboratories Report, 2017*, SAND2017-5378, Albuquerque, NM, 2017.

12. Harrington, R. F., *Time-harmonic Electromagnetic Fields*, Chapters 1, 5, 7, Wiley-IEEE Press, 2001.

13. ECCOSORB MCS, Emerson & Cuming Microwave Products, https://www.laird.com/rfmicrowave-absorbers-dielectrics/elastomers-films-foams/cavity-resonance-and-surface-wave-absorbers/eccosorb-mcs.